# A robust three-dimensional mesoporous Ag/$TiO_2$ nanohybrid film†

**Xinchen Wang, Jimmy C. Yu,* Chunman Ho and Angelo C. Mak**

*Received (in Cambridge, UK) 14th January 2005, Accepted 2nd March 2005*
*First published as an Advance Article on the web 14th March 2005*
**DOI: 10.1039/b500605h**

**A Ag/$TiO_2$ nanocomposite, in which silver nanoparticles are highly dispersed in the uniformly sized pores of a cubic mesoporous $TiO_2$ molecular-sieve film, has been fabricated.**

Metal/semiconductor composite systems have been extensively studied because of their unique catalytic and optoelectronic properties mainly determined by the size, morphology, composition, crystallinity and structure of the composites.[1] Among these systems, the well-known Ag/$TiO_2$ composite is extremely attractive owing to the intrinsic properties of $TiO_2$ and Ag. $TiO_2$ is the most widely used photocatalyst due to its powerful light-induced ability to degrade organic pollutants in both water and air, and to its nontoxicity, photostability and chemical inertness.[2] Silver nanoparticles are also widely studied in catalysis, photography, photonics, optoelectronics, chemical/biological labeling, and information storage.[3] The specific interactions between $TiO_2$ and Ag in the nanosized regime can indeed be responsible for the detection of new physical properties and for enhanced catalytic activity. The coupling with noble metals has also been demonstrated to increase the quantum yield of $TiO_2$ photocatalyst by significantly prohibiting the fast recombination of photogenerated charge carriers.[2]

Several synthetic approaches (*e.g.*, physical blending, chemical precipitation, photochemical/photocatalytic reduction) for realizing Ag/$TiO_2$ composites have been reported.[4] But the challenge of synthetically controlling the size, morphology and dispersion of metal clusters has been met with limited success.[5] Development of new synthetic routes to metal/oxide nanocomposites is therefore desirable and has received much attention. For instance, core-shell nanostructure of Ag/$TiO_2$ with controllable core diameter and shell thickness has been created.[6] In addition, $TiO_2$-nanorod-stabilized Ag nanoparticles have also been fabricated in a nonpolar homogeneous solution.[1c] Despite these advances, recent developments of nano- and mesosynthetic chemistry still offer unexploratory opportunities for the fabrication of novel Ag/$TiO_2$ composites.

Herein, we first use ordered mesoporous nanocrystalline $TiO_2$ film as a hard template to support Ag nanoparticles. The template possesses large surface area, uniform nanosized pores, and 3D periodic mesoarchitecture. This, combined with ultrasound-assisted insertion technology,[7] can generate a high dispersion of naked Ag nanoparticles stabilized by the $TiO_2$ mesonetwork itself. It can therefore avoid the use of undesirable organic stabilizers, which is often detrimental to catalytic performance of Ag/$TiO_2$ composites.

Mesoporous $TiO_2$ molecular-sieve film was synthesized by a surfactant-templated approach. Detailed synthetic information can be found elsewhere.[8] The deposition of Ag nanoparticles in the $TiO_2$ film is as follows. The $TiO_2$ film was immersed in a bottle filled with a solution of 20 mg $AgNO_3$ in 4 mL deionized water. The bottle was put in an ultrasonic cleaning bath and connected to a vacuum pump. After sonication with reduced pressure for 3–10 minutes, the bottle was stored in a vacuum oven for 12 h. The film was then washed gently with deionized water to remove the surface-adsorbed precursor. After drying at 30 °C under vacuum, the film was irradiated with UV light (254 nm) in the presence of methanol vapors for 2 h. This converted the Ag ions to Ag particles by $TiO_2$ photocatalysis. The amount of Ag can be simply controlled by using different concentrations of $AgNO_3$ or by repeating the inclusion process. The film is robust as it remains intact after sonication for as long as 30 min.

Fig. 1A shows nitrogen adsorption–desorption‡ isotherms (inset) and pore size distribution plots for the mesoporous $TiO_2$

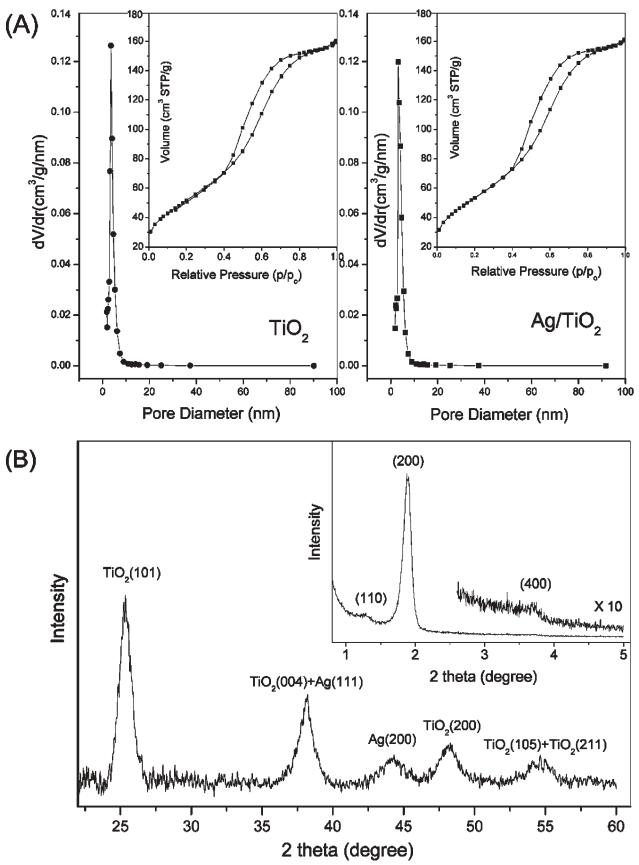


**Fig. 1** (A) $N_2$-sorption isotherms (inset) and corresponding pore-size distribution curves for pure $TiO_2$ and Ag/$TiO_2$, and (B) XRD patterns for Ag/$TiO_2$ in wide-angle and small-angle (inset) regions.

† Electronic supplementary information (ESI) available: SEM image of the Ag/$TiO_2$ nanohybrid film and its CO catalytic oxidation activity. See http://www.rsc.org/suppdata/cc/b5/b500605h/

*jimyu@cuhk.edu.hk

 

and Ag/$TiO_2$. Both samples show a type-IV isotherm, which is representative of mesoporous solids. The specific surface area of the Ag/$TiO_2$ composite is 195 $m^2$/g using the Brunauer–Emmett–Teller (BET) method. The pore diameter of the Ag/$TiO_2$ is 39 Å (estimated using the desorption branch of the isotherm) with very narrow pore size distribution. The $TiO_2$ possesses virtually identical average pore diameter (40 Å) and specific surface area (189 $m^2$/g), considering a typical uncertainty of $\pm 5\%$ for BET surface area measurements.[9] The addition of Ag causes a slight decrease, from 0.261 to 0.252 $cm^3$/g, in the pore volume of $TiO_2$. These results show that the deposition of Ag particles does not significantly change the textural properties of $TiO_2$, properly due to the small amount of Ag loaded. Thus, most of the pore channels in $TiO_2$ film are open, although a small portion of the channels may be filled with the Ag particles. Such open mesoporous architecture with large surface area and 3D connected pore-system is an important consideration in catalyst design because it can improve the molecular transport of reactants and products.[10]

The crystalline phase and mesostructural ordering of the Ag/$TiO_2$ composite film were characterized by both wide-angle X-ray diffraction (WXRD) and small-angle X-ray diffraction (SXRD§) measurements. As shown in Fig. 1B, SXRD exhibits several diffraction peaks at $2\theta$ of 25.3, 38.2, 44.2, 48.1, 53.5 and 55.6°. These peaks are attributed to anatase-$TiO_2$ (JCPDF 84-1285) and Ag (JCPDF 03-0921), as indexed in Fig. 1B. The particle size for the $TiO_2$ is 6 nm, whereas it is 5 nm for the Ag. These sizes were estimated from the fwhm of the $TiO_2$ (101) and Ag (200) peaks using the Sherrer formula. This indicates that both $TiO_2$ and Ag particles are nanocrystalline. The crystallization of the $TiO_2$ mesoporous framework is very important for applying the film in devices that utilize its semiconductor properties, such as photocatalysts. The crystalline structure of the $TiO_2$ explains partly the stability of the film under ultrasound irradiation. At the lower $2\theta$ region (Fig. 1B, inset), the XRD pattern is dominated by a strong peak at 1.8° ($2\theta$), with relatively weak peaks at 1.3 and 3.6°. These diffraction peaks can be indexed as (200), (110), and (400) reflections of a body-centered cubic mesophase. The sharp and strong (200) peak, together with the presence of the (400) peak, is an indication that the Ag/$TiO_2$ nanocomposite is well-organized in the meso scale. In addition, the relatively weak nature of the (110) reflection is due to the oriented growth of the film with the (100) plane parallel to the substrate. Similar oriented growth mesostructured silica and titania films have also been reported.[11]

The transmission electron microscopy (TEM¶) images support the wide- and small-angle XRD results. A long-range order structure is readily observed in the Ag/$TiO_2$ composite film (Fig. 2a). Combined with SXRD analysis, the image belongs to the (111) lattice plane of a body-centered cubic mesophase with a space group of $Im\bar{3}m$. The image also clearly shows that the Ag particles are highly dispersed in the framework of the mesoporous $TiO_2$. No large aggregation of the Ag particles on the surface of the film is observed. The high dispersion of metal particles in an active oxide (*e.g.* $TiO_2$) is a classic example of catalysts in which the catalytic performance of the metal component is strongly modified by interaction with the support. Fig. 2b is the high-resolution TEM image of the Ag/$TiO_2$ film. The nanocrystalline nature of both $TiO_2$ (solid circles) and Ag (dotted circles) is visibly observed in Fig. 2b.[12] This figure also confirms that Ag is adsorbed into the $TiO_2$ mesoporous network as nanoparticles. The $TiO_2$ and Ag nanocrystals of particle size $< 5$ nm are located close to each other, forming metal//semiconductor nanoheterojunctions. These nanoheterojunctions are known for causing Schottky-diode behavior of Ag contacts on $TiO_2$.[13] The Schottky-diode can significantly inhibit the fast recombination of electron–hole pairs on UV-excited $TiO_2$, improving photocatalytic efficiency.[2] The presence of Ag species on the mesoporous $TiO_2$ film is further confirmed by the electron dispersive X-ray spectroscopy investigation (Fig. 2c), which reveals a Ag/Ti element molar ratio of $\sim 0.05$.

The oxidation state of the Ag species is examined by X-ray photoelectron spectroscopy (XPS‖). Fig. 3a shows the XPS of Ag/$TiO_2$ composite film in the Ag $3d_{5/2}$ and Ag $3d_{3/2}$ binding energy regions. The Ag $3d_{5/2}$ peak is centered at 367.8 eV whereas the Ag $3d_{3/2}$ peak is found at 373.8 eV, with a spin energy separation of 6.0 eV. This is characteristic of metallic silver (Ag°).[14] The formation of Ag° nanoparticles is also substantiated by UV-vis absorption spectra**(Fig. 3b). A broad band at 430 nm

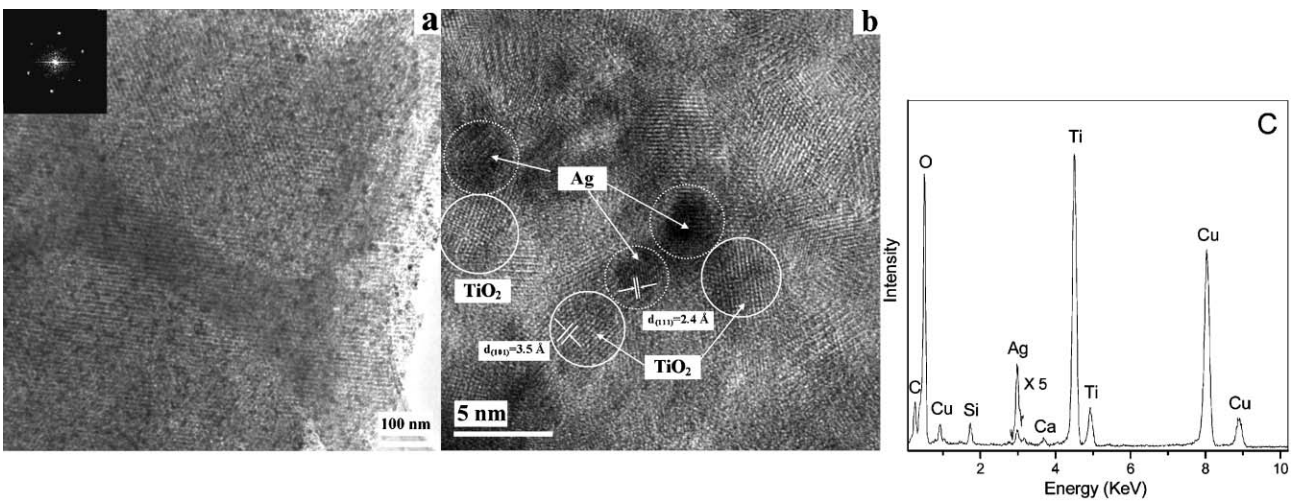


**Fig. 2** (a) Standard transmission electron microscopy (TEM), and (b) high-resolution TEM images of the Ag/$TiO_2$ composite film. The inset in (a) is the Fourier-transform of the selected area in (a). (c) is the energy dispersive X-ray (EDX) analysis of (a). Note: the Cu and C come from the supporting carbon-coated copper grid, and the Si and Ca come from the substrate.

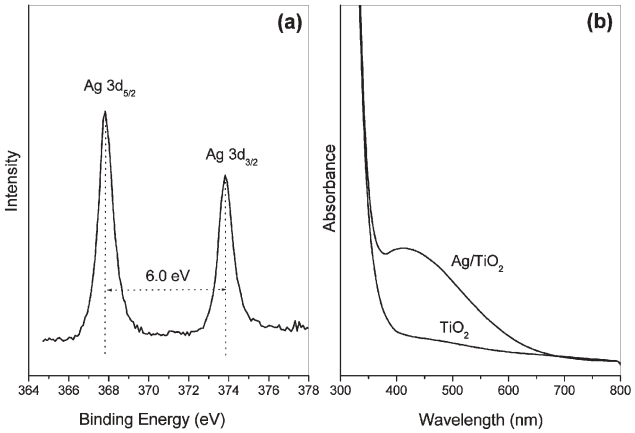


**Fig. 3** (a) X-ray photoelectron spectra of $Ag/TiO_2$ film in the Ag $3d_{5/2}$ and Ag $3d_{3/2}$ binding energy region. (b) UV-vis absorption spectra of $TiO_2$ and $Ag/TiO_2$ films.

appears on the UV-vis absorption spectra of $Ag/TiO_2$ composite film. This band is attributed to the surface plasmon resonance (SPR) of metallic silver nanoparticles in a $TiO_2$ matrix.[15] The strong SPR absorption of noble metals is well known for their applications in biochemical sensing and labeling devices.[16] The strong increase in absorption below 380 nm is caused by the band-gap absorption of the titania semiconductor, resulting from the excitation of electrons from the valence band to the conduction band of $TiO_2$.

In summary, the high dispersion of silver nanoparticles is readily realized by encapsulation in the pore channels of ordered mesoporous $TiO_2$ film. The resulting homogeneous and crack-free mesoporous $Ag/TiO_2$ nanoarchitecture (Fig. S1, ESI) possesses large specific surface area, uniform pore size, and a 3D accessible framework. The Ag particles are well confined in the pore channels and the particle size can be controlled to below 5 nm. Such porous architecture and dimensions are desirable features for catalytic and photocatalytic applications. Our preliminary results show that the $Ag/TiO_2$ film is active for catalytic oxidation of CO (Fig. S2, ESI). $Ag/TiO_2$ composite materials are also known to exhibit bactericidal activity.[17] These properties would make the novel nanohybrid film useful for automobile exhaust treatment and disinfection.

This work was supported by the Research Grants Council of the Hong Kong Special Administrative Region (Project No. 402904). We thank Mr Tze Kin Cheung of The Hong Kong University of Science and Technology for the TEM measurements and we appreciate the assistance of Dr Suk Yin Lai of the Hong Kong Baptist University in exploring the CO oxidation capability.

**Xinchen Wang, Jimmy C. Yu,* Chunman Ho and Angelo C. Mak**
*Department of Chemistry and Environmental Science Program, The Chinese University of Hong Kong, Shatin, New Territories, Hong Kong, China. E-mail: jimyu@cuhk.edu.hk; Fax: (+852) 2603-5057; Tel: (+852) 2609-6268*

## Notes and references

‡ Nitrogen adsorption–desorption isotherms were collected at 77 K using Micromeritics ASAP 2010 equipment.
§ WXRD and SXRD diagrams were collected in $\theta$–$\theta$ mode using a Bruker D8 Advance X-ray diffractometer (Cu $K\alpha_1$ irradiation, $\lambda$ = 1.5406 Å).
¶ TEM and high-resolution TEM were recorded on a JEOL 2010F microscope coupled with an electron dispersive X-ray (EDX) spectroscopy investigation. Carbon-coated copper grids were used as the sample holder.
‖ XPS measurements were done in a PHI Quantum 2000 XPS System with a monochromatic Al Kα source and a charge neutralizer; all the binding energies were referenced to the C 1s peak at 284.8 eV of the surface adventitious carbon.
** UV-vis absorption spectra were recorded with a Varian Cary 100 Scan UV-Visible system.

1 (*a*) T. Mokari, E. Rothenberg, I. Popov, R. Costi and U. Banin, *Science*, 2004, **304**, 1787; (*b*) Y. Ohko, T. Tatsuma, T. Fujii, K. Naoi, C. Niwa, Y. Kubota and A. Fujishima, *Nat. Mater.*, 2003, **2**, 29; (*c*) P. D. Cozzoli, R. Comparelli, E. Fanizza, M. L. Curri, A. Agostiano and D. Laub, *J. Am. Chem. Soc.*, 2004, **126**, 3868; (*d*) M. Valden, X. Lai and D. W. Goodman, *Science*, 1998, **281**, 1647.
2 M. R. Hoffmann, S. T. Martin, W. Choi and D. W.Bahnemann, *Chem. Rev.*, 1995, **95**, 69 and references therein.
3 (*a*) L. N. Lewis, *Chem. Rev.*, 1993, **93**, 2693; (*b*) D. M.-K. Lam and B. W. Rossiter, *Sci. Am.*, 1991, **265**, 80; (*c*) S. A. Maier, M. L. Brongersma, P. G. Kik, S. Meltzer, A. A. G. Requicha and H. A. Atwater, *Adv. Mater.*, 2001, **13**, 1501; (*d*) P. V. Kamat, *J. Phys. Chem. B*, 2002, **106**, 7729; (*e*) S. R. Nicewarner-Pena, R. G. Freeman, B. D. Reiss, L. He, D. J. Pena, I. D. Walton, R. Cromer, C. D. Keating and M. J. Natan, *Science*, 2001, **294**, 137; (*f*) C. B. Murray, S. Sun, H. Doyle and T. Betley, *Mater. Res. Soc. Bull.*, 2001, **26**, 985.
4 (*a*) Y. Tian and T. Tatsuma, *Chem. Commun.*, 2004, 1810; (*b*) D. S. Seo, H. Kim, H. C. Jung, J. K. Lee and A. Lee, *J. Mater. Res.*, 2003, **18**, 571; (*c*) H. Tada, T. Ishida, A. Takao and S. Ito, *Langmuir*, 2002, **20**, 7898.
5 Y. G. Sun and Y. N. Xia, *Science*, 2002, **298**, 2176.
6 R. T. Tom, A. S. Nair, N. Singh, M. Aslam, C. L. Nagendra, R. Philip, K. Vijayamohanan and T. Pradeep, *Langmuir*, 2003, **19**, 3439.
7 (*a*) A. Gedanken, X. Tang, Y. Wang, N. Perkas, Y. Koltypin, M. V. Landau, L. Vradman and M. Herskowitz, *Chem. Eur. J.*, 2001, **7**, 4546; (*b*) J. C. Yu, X. C. Wang, L. Wu, W. K. Ho, L. Z. Zhang and G. T. Zhou, *Adv. Funct. Mater.*, 2004, **14**, 1178.
8 J. C. Yu, X. C. Wang and X. Z. Fu, *Chem. Mater.*, 2004, **16**, 1523.
9 (*a*) F. Rouquerol, J. Rouquerol and K. Sing, *Adsorption by Powders and Porous Solids*, Academic Press, Sydney, 1999; (*b*) A. Badalyan and P. Pendleton, *Langmuir*, 2003, **19**, 7919.
10 (*a*) D. R. Rolison, *Science*, 2003, **299**, 1698; (*b*) A. T. Bell, *Science*, 2003, **299**, 1688.
11 (*a*) D. Zhao, P. Yang, N. Melosh, J. Feng, B. F. Chemlka and G. D. Stucky, *Adv. Mater.*, 1998, **10**, 1380; (*b*) C. A. Alberius, K. L. Frindell, R. C. Hayward, E. J. Kramer, G. D. Stucky and B. F. Chmelka, *Chem. Mater.*, 2002, **14**, 3284.
12 Due to the difference in contrast of $TiO_2$ and Ag particles, the TEM images of Ag are much darker than that of $TiO_2$. Moreover, the lattice fringes appearing in Fig. 2b also allow positive identification of the two species. The fringes of $d$ = 3.5 Å and $d$ = 2.4 Å calculated from Fig. 2b match that of the (101) and (111) crystallographic planes of anatase-$TiO_2$ and the Ag cubic phase.
13 K. D. Schierbaum, S. Fischer, M. C. Torquemada, J. L. de Segovia, E. Roman and J. A. Martin-Gago, *Surf. Sci.*, 1996, **345**, 261.
14 J. F. Moulder, W. F. Stickle, P. E. Sobol and K. D. Bomben, *Handbook of X-ray Photoelectron Spectroscopy*, (Ed.: J. Chastain), Perkin-Elmer Corporation, USA, 1992, p. 182.
15 J. H. He, I. Ichinose, S. Fujikawa, T. Kunitake and A. Nakao, *Chem. Commun.*, 2002, 1910.
16 N. Nath and A. Chilkoti, *Anal. Chem.*, 2004, **76**, 5370.
17 L. Z. Zhang, J. C. Yu, H. Y. Yip, Q. Li, K. W. Kwong, A. W. Xu and P. K. Wong, *Langmuir*, 2003, **19**, 10372.

 